Applied Surface Science 254 (2008) 7950–7954

Contents lists available at ScienceDirect

Applied Surface Science

journal homepage: www.elsevier.com/locate/apsusc

An extreme change in structural and optical properties of indium oxynitride deposited by reactive gas-timing RF magnetron sputtering

A. Sungthong [a,c,*], S. Porntheeraphat [b], A. Poyai [b], J. Nukeaw [a,c]

[a] Nanotechnology Research Center of KMITL, King Mongkut's Institute of Technology Ladkrabang, Bangkok 10520, Thailand
[b] Thai Microelectronics Center, National Electronics and Computer Technology Center, Pathumthani 12120, Thailand
[c] Department of Applied Physics, King Mongkut's Institute of Technology Ladkrabang, Bangkok 10520, Thailand

ARTICLE INFO

Article history:
Available online 2 June 2008

PACS:
68.55.Jk
68.37.Ps
61.66.Dk
61.10.Nz

Keywords:
Indium nitride
Indium oxynitride
Indium oxide
Reactive gas-timing
RF magnetron sputtering

ABSTRACT

The indium oxynitride (InON) films were achieved by reactive RF magnetron sputtering indium target which has the purity of 99.999% with a novel reactive gas-timing technique. The structural, optical and electrical properties in a series of polycrystalline InON films affected by gas-timing of reactive N_2 and O_2 gases introduced to the chamber were observed. The X-ray photoelectron spectroscopy revealed that the oxygen content in thin films that compounded to indium and nitrogen, which increased from 10% in indium nitride (InN) to 66% in indium oxide (In_2O_3) films. The X-ray diffraction peaks show that the phase of deposited films changes from InN to InON and to In_2O_3 with an increasing oxygen timing. The hexagonal structure of InN films with predominant (0 0 2) and (0 0 4) orientation was observed when pure nitrogen is only used as sputtering gas, while InON and In_2O_3 seem to demonstrate body-center cubic polycrystalline structures depending on gas-timing. The surface morphologies investigated from atomic force microscope of deposited films with varying gas-timing of O_2:N_2 show indifferent. The numerical algorithm method was used to define the optical bandgap of films from transmittance results. The increasing oxygen gas-timing affects extremely to the change of crystallinity phase from InN to InON and to In_2O_3, the increase of optical bandgap from 1.4 to 3.4 eV and the rise of sheet resistance from 15 Ω/□ to insulator.

© 2008 Elsevier B.V. All rights reserved.

1. Introduction

Indium oxynitride (InON) is relatively a new class of material which is very useful and its effective optical, electrical and mechanical properties have a great potential for industrial applications. A numerous property of InON film, for example, refractive index and dielectric constant of this film by varying the proportion between oxygen and nitrogen which are contained in the film is formed. Furthermore, by depositing such oxynitride film on a semiconductor surface, it is possible to use it as a surface passivation film as well [1]. The high air–InN and/or high oxide/InN contrast in refractive index is therefore very attractive for photonic bandgap design [2]. Recently, there just have been a few researches on InON films. InON nanoparticles were synthesized on a silicon substrate in nitrogen atmosphere using the method involving thermal evaporation of pure indium in a two-zone reactor [3]. It was found that with increasing growth temperatures there was not only the formation of high quality InON nanoparticles but also an increase in the intensities of emissions. The mechanisms of reactive sputtering growth of InON in mixed N_2–O_2 discharges were reported [4].

Our innovative reactive gas-timing technique for RF magnetron sputtering was applied successfully to achieve nitride and oxide films including AlN, InN, and ITO with good structural and optical properties [5,6]. The reactive gas-timing is a technique to control the sequence of gas fed into the sputtering chamber to yield the nitride, oxynitride and oxide films.

In the present study, we report an experimental study of the relationship between the structural, optical bandgap and electrical properties of InON series grown by reactive gas-timing technique using RF magnetron sputtering. The details of experimental growths and characterizations will be discussed.

2. Experimental details

A series of InN–InON–In_2O_3 thin films were deposited using RF magnetron sputtering with the reactive gas-timing technique on glass substrate. A diagram of reactive gas-timing is presented in

* Corresponding author at: Nanotechnology Research Center of KMITL, King Mongkut's Institute of Technology Ladkrabang, Bangkok 10520, Thailand.
E-mail address: s9067001@kmitl.ac.th (A. Sungthong).

0169-4332/$ – see front matter © 2008 Elsevier B.V. All rights reserved.
doi:10.1016/j.apsusc.2008.04.038

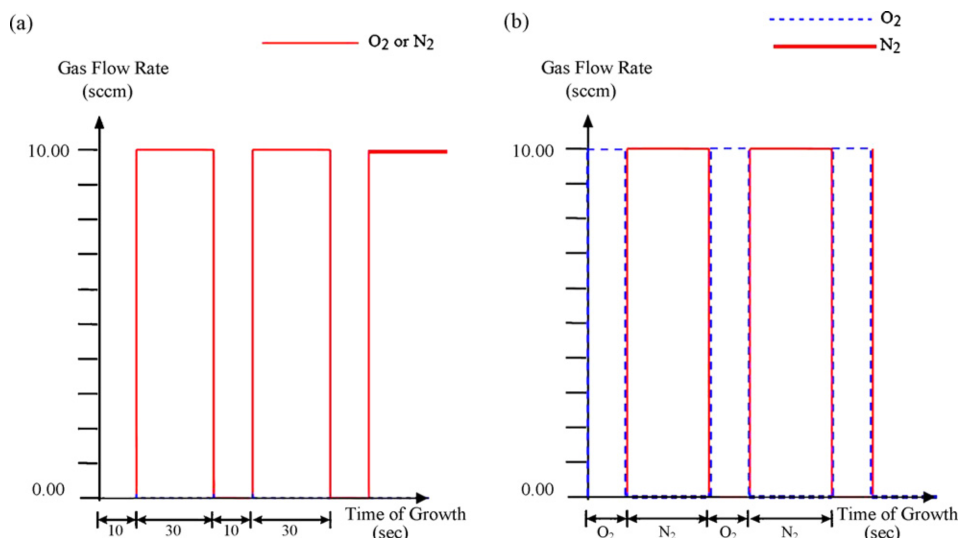

Fig. 1. A diagram of reactive gas-timing fed into the chamber: (a) O_2 or N_2 and (b) O_2:N_2.

Table 1
Deposition parameters of InON thin films

Target	99.999% Indium (In), 3 in. diameter
Substrate	Borosilicate glass
Substrate distance	7 cm
Holder speed	30 rpm
Base pressure	2×10^{-7} mbar
RF power	100 W
Gas flow rate (O_2:N_2)	10:10 sccm
Thickness	500 nm
Deposition rate (O_2:N_2)	0.06:0.14 nm/s
Gas-timing (O_2:N_2)	N_2-timing, 10:30, 20:30, 30:30 and O_2-timing (s)

Fig. 1. Fig. 1(a) shows timing diagram of O_2 or N_2 flow sequence for depositing In_2O_3 or InN thin films. The period of gas (O_2 or N_2) on is 30 s, while off is 10 s. Fig. 1(b) shows timing diagram of O_2:N_2 in the ratio of 10:30, 20:30, 30:30 s for deposited InON films. The deposition parameters of film series are shown in Table 1. The substrate was kept at room temperature during the deposition.

The oxygen content, structural, optical characterizations and sheet resistant measurement were investigated by X-ray photo-electron spectroscopy (XPS), X-ray diffraction (XRD), atomic force microscope (AFM), UV–vis spectroscopy (UV–vis) and standard four-point probe instrument, respectively.

3. Results and discussions

A series of InN–InON–In_2O_3 films exhibit difference in color in range between dark brown and clearly transparent as shown in Fig. 2. The %oxygen content achieved from XPS in InN–InON–In_2O_3 films grown with different O_2:N_2-timings is shown in Fig. 3. As the O_2-timing was further increased, the %oxygen exceeded from 10% to 66% contented in InN–InON–In_2O_3 film series.

It can be seen that the oxygen content is lowest at 10% in film sputtered with pure N_2 (N_2-timing). The oxygen composition in sputtered-film from pure N_2 plasma that caused by an unavoidable residual agent (O_2) in the vacuum system at base pressure of about 10^{-7} mbar and the higher reactivity of oxygen in the reactor which compared to nitrogen. These suggestions can imply the oxygen contamination in deposited film without feeding O_2 gas into the vacuum chamber. An increasing oxygen concentration was observed corresponding to the increase of O_2-timing caused by the decrease of nitrogen.

Fig. 4 shows typical XRD patterns of InN–InON–In_2O_3 films deposited at different timings of O_2:N_2. The deposited film with 30 s (on–off N_2-timing), shows very strong peak preferred (0 0 2) orientation indicating the *c*-axis of the hexagonal InN structure perpendicular to the substrate [7–10], while the diffraction peaks at 35.46° and 51.04° reveal (4 0 0) and (4 4 0) as a body-center cubic structure of In_2O_3. The films sputtered with O_2:N_2-timing of

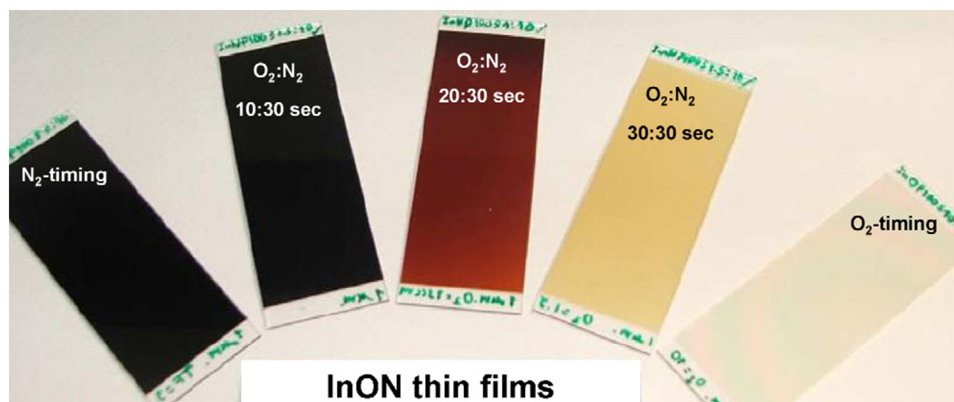

Fig. 2. Exhibit difference in color in range between dark brown and clearly transparent.

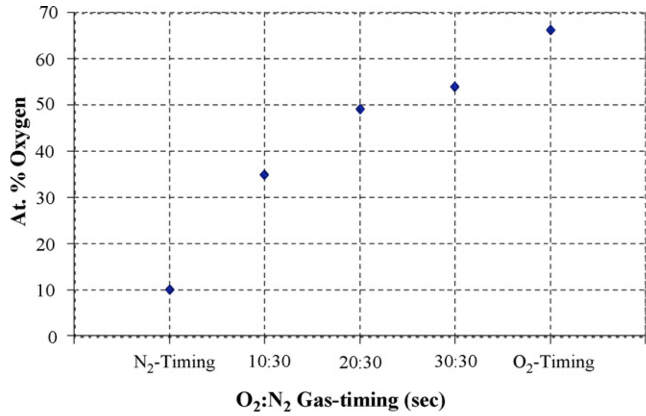

Fig. 3. The %oxygen obtained from sputtered InON films with gas-timing of O_2:N_2 in the ratio of N_2-timing, 10:30, 20:30, 30:30 and O_2-timing (s), respectively.

10:30, 20:30 and 30:30 s, showed obviously change in crystalline phase. Its diffraction peaks match tabulated values for InN [11].

The oxynitride formation was observed in InN film deposited by dc reactive magnetron sputtering by post-treatment of these films in N_2 [12], and a series of films were obtained with compositions gradually going from as prepared InN (1 0 1) into fully oxidized In_2O_3 (2 2 2).

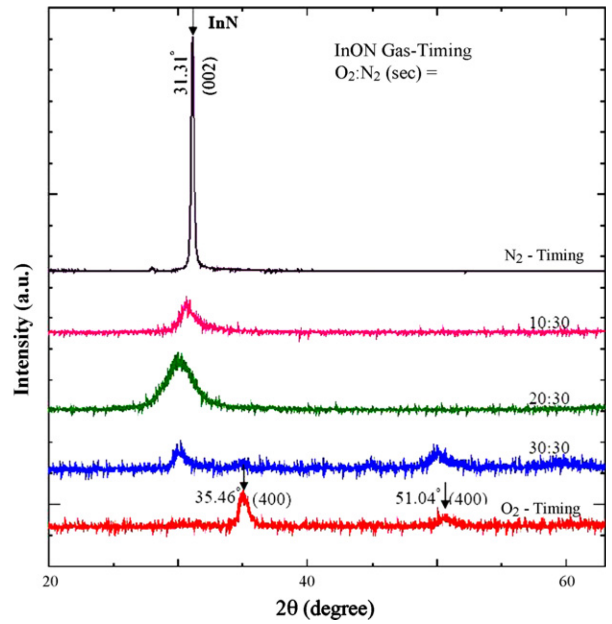

Fig. 4. X-ray diffraction profile of the InN–InON–In_2O_3 series with gas-timing of O_2:N_2 in the ratio of N_2-timing, 10:30, 20:30, 30:30 and O_2-timing (s).

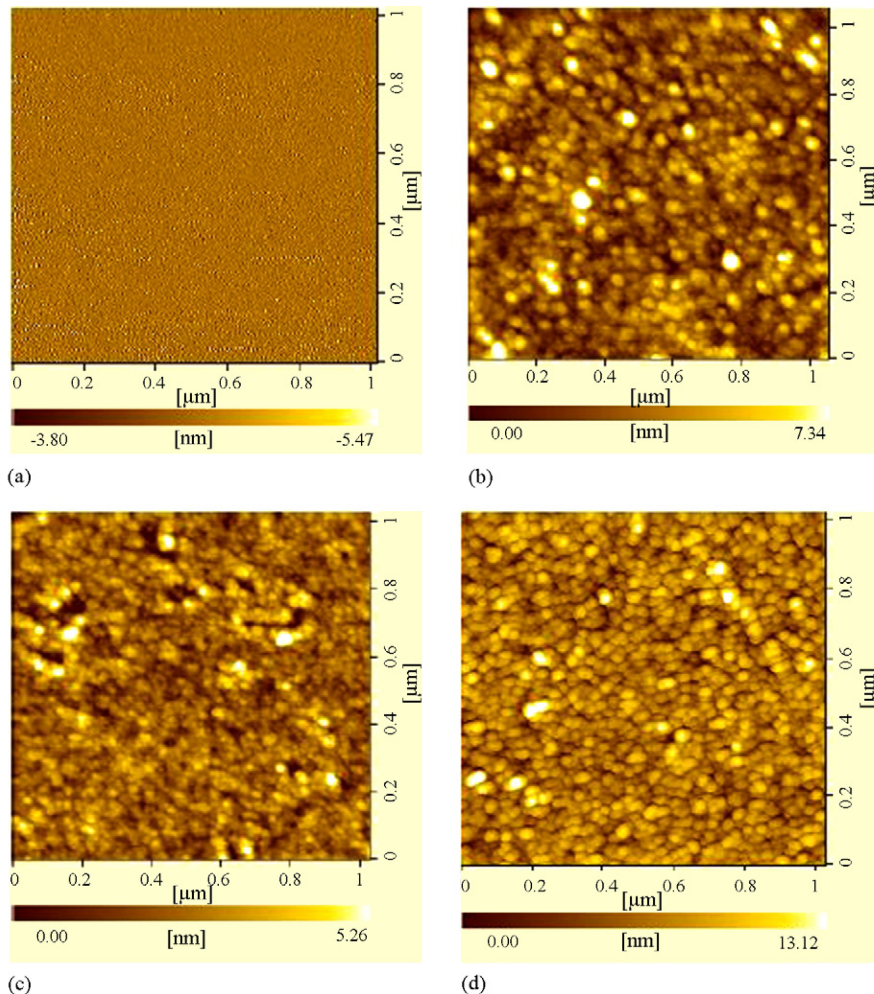

Fig. 5. AFM images of InON film series deposited at O_2:N_2-timing of (a) N_2-timing, (b) 10:30, (c) 30:30 and (d) O_2-timing.

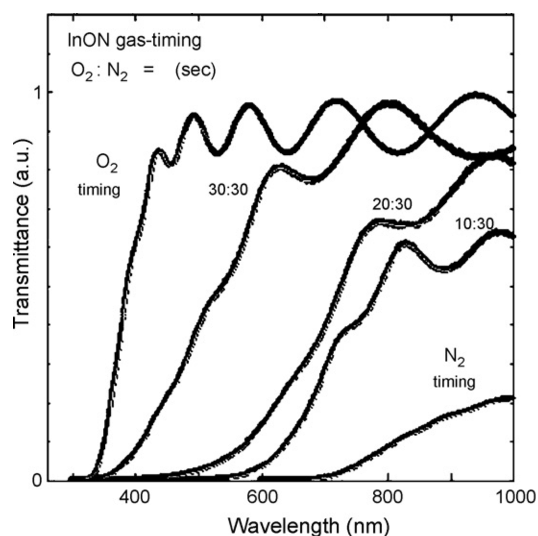

Fig. 6. The optical transmission spectra of InON thin film series with different gas-timings of O_2:N_2 used as sputtering gas.

The diffraction peaks of our samples shift from InN to InON and to In_2O_3 phase corresponding to %oxygen content obtained from XPS investigation.

The surface morphology obtained by AFM of InN–InON–In_2O_3 series deposited on glass substrate with different timings of O_2:N_2 is shown in Fig. 5. The surface morphology of the sample grown with only N_2-timing shows very smooth grains (Fig. 5(a)) and gradually consists of rounded grains as shown in Fig. 5(b)–(d). From the results of AFM, the oxygen has a strong influence on the surface morphology of film. The surface became rough when the oxygen increases as shown in Fig. 5(a) revealed a rms roughness of 1.058 nm and Fig. 5(b) revealed a rms roughness of 1.457 nm. The higher value of roughness may be due to oxygen compositions that lead to increase in both the amount of amorphous material and void fraction [13].

The optical transmittance of the films was measured with double beams spectrophotometer, scanned in the UV–vis region (300–1000 nm). The optical transmission spectra of InN–InON–In_2O_3 thin film series with different gas-timings of O_2:N_2 show that the film transmittance changes substantially, as shown in Fig. 6. There is extremely different of transparent spectrum depending on O_2:N_2.

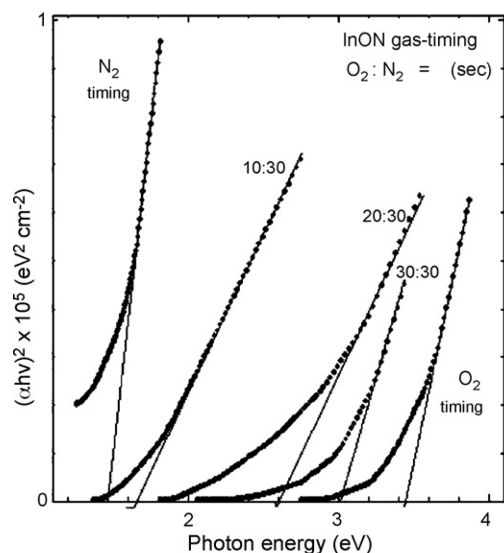

Fig. 7. The InON film series grown in different timings of O_2:N_2.

Table 2
The sheet resistance of InN–InON–In_2O_3 film series measured from four-point probe technique

Gas-timing O_2:N_2 (s)	Sheet resistance (Ω/□)
N_2-timing	15.29
10:30	83.61
20:30	1.251
30:30	2×10^6
O_2-timing	Insulator

The optical bandgap in a series of InN–InON–In_2O_3 films determined by numerical algorithms methods, pointwise unconstrained optimization approach (PUMA), for fitting from transmittance spectrum, as displayed in Fig. 7. The optical bandgap of InN–InON–In_2O_3 film series grown in different timings of O_2:N_2 are achieved in value of 1.4–3.4 eV.

It has been proposed that the large discrepancy between the previously measured large bandgap of InN (~1.9 eV) and the recently discovered narrow bandgap could be due to the formation of indium oxynitride alloys in older sputter-grown films, since sputtered films often contained high levels of oxygen contamination that can be over 10% in some extreme cases [10,12]. Assuming a linear composition dependence of the direct bandgap of the alloy formed by InN and In_2O_3 [11,14].

Normally, the oxynitride phase observed in InN thin films occurred with oxygen contamination in the system or post-processes. The annealing of InN thin film after the sputtering process is a method to introduce the oxygen incorporation with InN. The oxygen concentration is increased as the annealing temperature is risen [12,14]. Instead of oxygen gaining from post-annealing like any other researches, our prepared thin films obtained oxygen composition through feeding on purpose in order to achieve InON thin films.

The sheet resistant of InN–InON–In_2O_3 film series measured from four-point probe technique is shown in Table 2. In our experiment, the increase of O_2-timing causes the increasing sheet resistance of films due to the rise of oxygen content. The sheet resistance of the investigated samples was in the range of 15 Ω/□ to insulator.

The low resistivity indicates a high density of charge carriers (in accordance with the NIR absorption) and band conduction rather than hopping as the dominant mechanism for charge transport. The resistivity values for InN has been reported before [15]. The oxygen concentration in the deposited films effects directly to the optical bandgap energy of films [16].

Surprisingly, the change of film composition by varying the gas-timing sequence of O_2:N_2 causes significant change in the crystalline structure, optical bandgap and sheet resistance. The experimental results clearly indicate that the gas-timing technique in sputtering growth plays an important role in the properties of InON films which are very attractive for material bandgap design.

4. Conclusion

The InON films with a wide range property were successfully achieved from a novel reactive gas-timing RF magnetron sputtering without substrate heating and post-annealing. The different O_2:N_2 gas-timing feeding to sputtering process affecting the structural, optical and electrical properties in a series of polycrystalline InON films was reported. The oxygen content in these films revealed by XPS increased from 10% to 66% depending on O_2:N_2-timing.

The XRD peaks show that the phase of deposited films changes from InN to InON and to In_2O_3 with an increasing O_2-timing. The hexagonal structure of InN films with predominant (0 0 2) and (0 0 4) orientation was observed when pure nitrogen is only used as sputtering gas while, InON and In_2O_3 demonstrate body-center cubic polycrystalline structures. The optical bandgap of these films strongly depends on O_2:N_2-timing and varies between 1.4 and 3.4 eV. The sheet resistance of InN–InON–In_2O_3 films was in the range of 15 $\Omega/\square$ to insulator. All measurement results are agreed together.

The results of our experiment clearly indicate that the reactive gas-timing technique applied for sputtering growth plays an important role in the formation of InN–InON–In_2O_3 crystalline. The advantage of the gas-timing method compared with that of the reactive RF magnetron sputtering technique using mixed gas was described in Refs. [5] and [6]. The wide range properties of InON films make them very attractive for material bandgap design and various applications.

Acknowledgements

The authors are grateful to National Electronics and Computer Technology Center (NECTEC) for the research grant no. NT-B-06-4A-22-314 and Faculty of Science, King Mongkut's Institute of Technology Ladkrabang, Thailand for the research facilities. This work also has been supported by the National Nanotechnology Center (NANOTEC), Ministry of Science and Technology, through program of Center of Excellence Network.

We also would like to thank the Thailand Graduate Institute of Science and Technology (TGIST), NECTEC for student fund supported no. TG-44-22-49-093D.

References

[1] United States Patent 4,416,952.
[2] K.S.A. Butcher, T.L. Tansley, Superlattice Microstruct. 38 (2005) 1–37.
[3] T.S. Ko, C.P. Chu, H.G. Chen, T.C. Lu, H.C. Kuo, S.C. Wang, J. Vac. Sci. Technol. A: Vac. Surf. Films 24 (July (4)) (2006) 1332–1335.
[4] B.R. Natarajan, A.H. Eltoukhy, J.E. Greene, T.L. Barr, Thin Solid Films 69 (16 June (2)) (1980) 217–227.
[5] N. Kietpaisalsophon, W. Bunjongpru, W. Techitdheera, J. Nukeaw, Int. J. Mod. Phys. B 16 (20 November (28 & 29)) (2002) 4418–4422.
[6] A. Klamchuen, N. Pornteeraphat, J. Nukeaw, e-J. Surf. Sci. Nanotechnol. 3 (2005) 272–275.
[7] B.D. Cullity, Elements of X-ray Diffraction, Addison-Wesley, Reading, MA, 1959.
[8] I. Chambouleyron, S. Ventura, E.G. Birgin, J.M. Martínez, J. Appl. Phys. 92 (2002) 3093–3102.
[9] O. Tskai, J. Ebisawa, Y. Hisamatsu, in: Proceedings of the Seventh International Conference on Vacuum Metallurgy, Tokyo, Japan, November 26–30, (1982), p. 129.
[10] N. Asai, Y. Inoue, H. Sugimura, O. Takai, Thin Solid Films 332 (1998) 267.
[11] Q. Guo, N. Shingai, Y. Mitsuishi, M. Nishio, H. Ogawa, Thin Solid Films 343–344 (1999) 524.
[12] O. Takai, K. Ikuta, Y. Inoue, Thin Solid Films 318 (1998) 148.
[13] R.E. Tanner, A. Szekeres, D. Gogova, K. Gesheva, Appl. Surf. Sci. 218 (2003) 162–168.
[14] M. Winterbert-Fouquet, K. Butcher, Motlan, Phys. Stat. Sol. (c) 0 (2003) 2785.
[15] Y. Sato, S. Sato, J. Cryst. Growth 146 (1995) 262.
[16] Motlan, E.M. Goldys, T.L. Tansley, J. Cryst. Growth 241 (2002) 165.